

The Intermolecular Charge-Transfer Complexes of the First Generation of poly(propylene amine) Dendrimers with σ and π Acceptors

Mohamed Y. El-Sayed^{1*,2} and Moamen S. Refat^{3,4}

¹ Department of Chemistry, Faculty of Science, Zagazig University, Egypt

² Faculty of Applied Medical Science, Al Jouf University-Al Qurayate

³ Chemistry Department, Faculty of Science, Taif University, P.O. Box 888, Al-Hawiah, Taif 21974, Saudi Arabia

⁴ Department of Chemistry, Faculty of Science, Port Said, Port Said University, Egypt

*E-mail: iyosri@yahoo.com

Received: 27 June 2014 / Accepted: 4 August 2014 / Published: 25 August 2014

The present paper was discussed to find out the public perception of the nature of charge transfer bonding between the first generation of poly(propylene amine) dendrimer (PPD) and like each of π and σ - acceptors. Iodine and picric acid (PA) were chosen because of them considered the most common of the receptors in the field of charge transfer complexes. The charge-transfer interaction of the PPD electron donor and the PA π -electron acceptor has been studied in CHCl_3 . The resulted data referred to the formation of the new CT-complex with the general formula $[(\text{PPD})(\text{PA})_2]$. The 1:2 stoichiometry of the reaction was discussed upon the on elemental analysis and photometric titration. On the other hand, the 1:2½ iodine-PPD pentaiodide (I_5^-) charge-transfer complex has been studied spectrophotometrically in chloroform at room temperature with general formula $[(\text{PPD})]^+\text{I}_5^-$. The electronic absorption bands of I_5^- are observed around ~ 360 and ~ 290 nm. Raman laser spectrum of the brown solid pentaiodide complex has two clearly vibration bands at 146 and 111 cm^{-1} due to symmetric stretching $\nu_s(\text{I-I})$ outer and inner bonds, respectively of the linear I_5^- ion with $\text{D}_{\infty\text{h}}$ point group. The electronic absorptions, infrared and Raman laser spectra, thermal analysis (TG/DTG/DSC), photometric titrations as well as elemental analysis of the resulted picric acid and iodine-PPD complexes were discussed.

Keywords: Dendrimer; pentaiodide; spectrophotometrically; picric acid; Raman laser

1. INTRODUCTION

The dendrimers are new attractive class of macromolecule having different functional groups in their core and periphery [1-3]. The introduction of fluorescent and photoactive chromophores into the

dendrimer molecules has been among the recent advancement of the dendrimer chemistry research. In recent years, fluorescent compounds comprising different chemical structure have been investigated as chemosensors [4]. The utilization of 1,8-naphthalimide derivatives as fluorescent sensor is based upon the fact that in protonated solution or in the presence of metal cations these compound display high photoinduced electron transfer (PET) resulting in the "off-on switching" of fluorescence [5]. Thus the luminescent dendrimer have been attaining great importance due to their applicability in high technology, especially in optoelectronics, light-harvesting antenna system for solar energy conversion, sensors for environmental pollutants, in biology and medicine [6-8]. The fluorescent photoinduced electron transfer (PET) sensors are of great interest because of their versatile application. Under appropriated conditions the fluorophore emission is quenched by the distal amine group with at least a partial electrontransfer proceeding from the amine group to the fluorophore ring. If the PET process is "switched off" by e.g protonation of amine or by their complexation the fluorescence of fluorophores is restored [9].

Poly(propylene amine) (PPA) is a new class of commercial dendrimers possessing tertiary amino groups in the core and terminal primary amino groups in the dendrimer periphery [10]. Each generation comprises 2^{n+1} tertiary amino groups in the interior and $2^{n+1}-2$ peripheral functional groups, where n is the number of generation. The photophysical properties of poly(propylene amine) dendrimers functionalized with dansyl or azobenzene units at the periphery have been investigated [11-17]. These dendrimers can coordinate metal ions by aliphatic amine units contained in the interior of the dendrimer and can be used as fluorescent sensors for metal ions such as Cu^{2+} and Zn^{2+} [18]. The advantage of these multichromophore systems is that a single analyte can interact with a great number of fluorescent units, which results in signal amplification. Furthermore, the interaction of fluorophores with one another and with other components of the dendrimer can result in new properties i.e. dendritic effect. For example three types of emission bands are registered in the spectra of such multichromophoric macromolecules, assigned to monomer, excimer and exciplex species.

Charge-transfer complexes using different organic species are intensively studied because of their special type of interactions, which accompanied by transfer of an electron from the donor to the acceptor [19-27]. The polyiodide ions like I_3^- , I_5^- , I_7^- and I_9^- were synthesized by the reactions of iodine as sigma acceptor with different organic (aliphatic/aromatic) donors such as amines and crown ethers which have interesting electronic and solar cells applications [28-35]. There are no reported data in literature survey on the intermolecular charge-transfer complexes of iodine or picric acid with poly(propylene amine) dendrimers except for our two published papers dealing with poly(amidoamine) dendrimers [36, 37]. Our recent research was focused on the charge-transfer chelation behavior of two different acceptors (iodine and picric acid) with poly(propylene amine). This study is also of great significance in improving the efficiency of fluorescent pigmentation and increased stability for use in solar cells.

2. EXPERIMENTAL

2.1. Materials

DAB-dendr-4Am dendrimer and 1,8-naphthalic anhydride, iodine, picric acid and other chemicals and solvents were received from Fluka, Aldrich and Merck companies, and used without further purification.

2.2. Materials

The first generations PPD dendrimer modified with 1,8-naphthalimide (Fig. 1) has been synthesized previously [38, 39] as follows:

The 0.65 mL (0.002M) of DAB-dendr-4Am was reacted with excess of 1,8-naphthalic anhydride in 50 mL ethanol. The reaction mixture was refluxed and heated for two hours at 80 °C. Afterwards the solution was poured into 200 mL water and the resulting precipitate was filtered off, washed with water and dried to a constant weight. In order to remove the unreacted 1,8-naphthalic anhydride, the precipitate was treated with 20 ml 5 wt% NaOH solution. Thus the unreacted 1,8-naphthalic anhydride was dissolved and removed after filtration while the modified poly(propylene amine) remained as the precipitate. Yield: 53.8%.

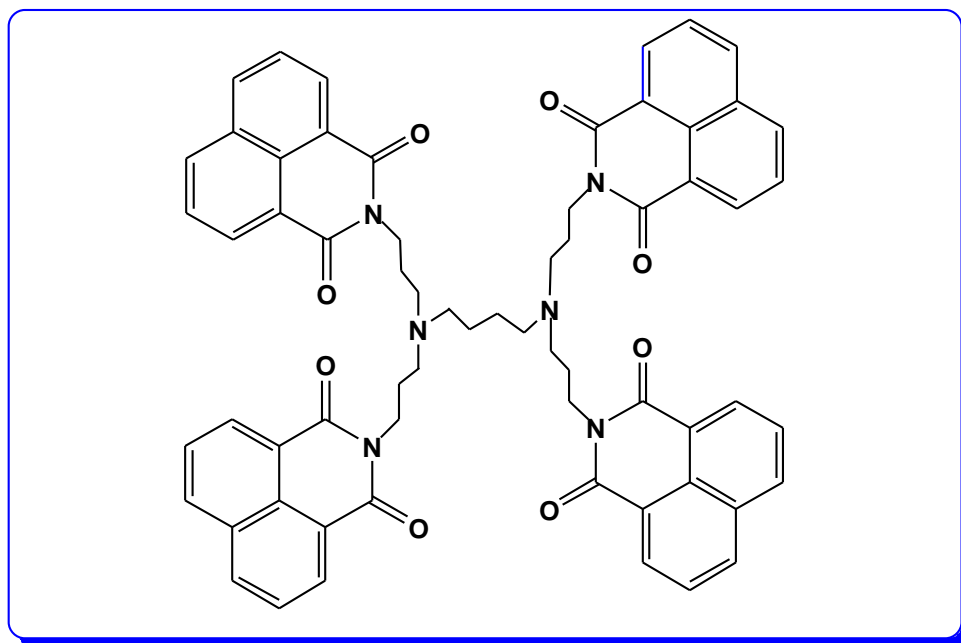


Figure 1. Chemical structure of poly(amidoamine) dendrimer (PPD).

2.3. Synthesis of I_2 and PA solid complexes

Both of solid charge-transfer complexes of PPD with σ -acceptor (I_2) and π -acceptor (PA) were prepared by mixing (0.1 mmol; 0.104 g) of the PPD donor in 20 mL chloroform with 0.2 mmol of each acceptor in the same solvent with continuously stirring for about 3 hr at room temperature 25 °C. The mixtures were allowed to evaporate slowly at room temperature, the resulted colored complexes in the

solid state was filtered and washed with little amount of solvent, finally dried under vacuum over anhydrous calcium chloride. Analysis: The dark brown $[(PPD)]^+I_5^-$ complex with empirical formula $C_{64}H_{56}O_8N_6I_5$; %C, 45.38(45.86); %H, 3.20(3.34); and %N, 5.15(5.02). Analysis: The yellow solid $[(PPD)(PA)_2]$ charge transfer complex with empirical formula $C_{76}H_{62}O_{22}N_{12}$; %C, 45.38(60.87); %H, 3.20(4.14); and %N, 5.15(11.21) (theoretical values are shown in brackets and experimental data without brackets).

2.4. Instrumentals

Elemental analyses were performed using a Perkin-Elmer CHN 2400 elemental analyzer. Molar conductance measurements of the PPD and their charge-transfer complexes with 1.0×10^{-3} mol/L in DMSO were carried out using Jenway 4010 conductivity. 1H -NMR spectra recorded using Varian 200 MHz Spectrometer with DMSO as solvent, chemical shift are given in ppm relative to tetramethylsilane. The UV/vis. spectra were obtained in chloroform solvent (1.0×10^{-4} M) for the reactants and products with a Jenway 6405 Spectrophotometer using 1 cm quartz cell, in the range 200–600 nm. IR spectra (4000 – 400 cm^{-1}) were recorded as KBr pellets on Bruker FT-IR Spectrophotometer, while Raman laser spectra of samples were measured on the Bruker FT-Raman with laser 50 mW. Thermogravimetric analyses (TG/DTG) were carried out in the temperature range from 25 to 800 °C in a steam of nitrogen atmosphere using Shimadzu TGA 50H thermal analysis, the experimental conditions were: platinum crucible, nitrogen atmosphere with a 30 ml/min flow rate and a heating rate 10 °C min^{-1} . The differential scanning calorimetry (DSC) was carried out using Delta Series DSC7 with scanning rate 10 °C min^{-1} .

3. RESULTS AND DISCUSSION

The growing color between iodine and picric acid acceptors with PPD donor were comprehensively spectrophotometrically studied to detect the optimal conditions for chelation process. The PPD has threetwo type of nitrogen donation atoms (Fig. 1), so it is act as a powerful electron donor. The two types of nitrogen atoms one of them as amide group which involved in the naphalimide moiety (flanked between two carbonyl groups) and the other nitrogen atoms is a tertiary with sp^3 hybridization type. The percentage of carbon, hydrogen and nitrogen elements are agreement with the 1:2 for PPD-PA and 1:2½ for PPD- I_5 molar ratios between PPD donor and some interesting acceptors like PA and iodine. The conductivity measurements of starting materials and resulted PPD charge transfer complexes were performed in DMSO with 1.0×10^{-3} mol/L concentration. The molar conductivities values of PPD charge-transfer complexes ranged within 35-50 $\Omega^{-1}cm^{-1}mol^{-1}$. The molar conductance data refereed to slightly electrolytic nature. This data are due to the formation of intermolecular positive and negative datives anions ($D^+—A^-$) under the acid-base theory [36, 37].

3.1. Electronic spectra

Figure 2 show the UV-vis electronic spectrum of PPD-I₂ system in CHCl₃ that is referred to both detected absorption bands at about ~ 360 and 295 nm which don't exist for any of the reactants. The photometric titration curve of the PPD-I₂ reaction based on the 360 nm absorption band is shown in Fig. 3. The molar ratio of PPD-I₂ reaction clearly indicates that the PPD: I₂ is 1:2½ and the intermolecular charge-transfer complex can be formulated as [(PPD)]⁺.I₅⁻. This resulted was matched with the elemental analysis and Raman laser discussions. According to the literature survey [28-31] the presence of common absorption bands at 360 and 295 nm were assigned to the formation of one type of polyiodide molecules I_n⁻ (where n= 1, 3, 5, 7, 9, ...). The polyiodide I₅⁻ charge-transfer complex resulted from our paper is agreement with the formation of (TMA)₁₀H⁺I₅⁻ (TMA= trimesic acid) and (CH₃)₄N⁺ I₅⁻ polyiodide charge transfer-complexes [28].

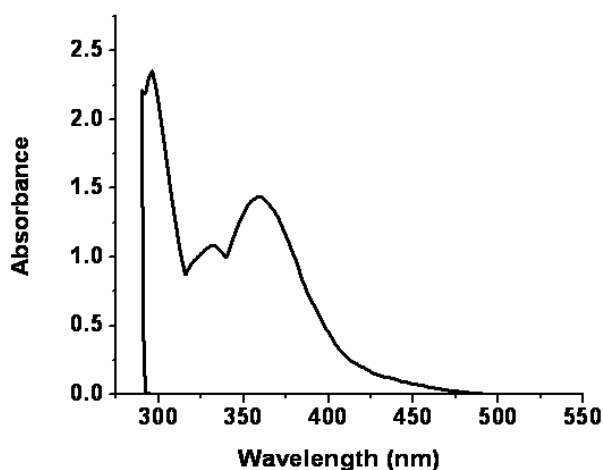


Figure 2. UV-vis absorption spectrum of PPD-I₂ system in CHCl₃ (PPD = 1.0×10⁻⁴ M and I₂ = 1.0×10⁻⁴ M).

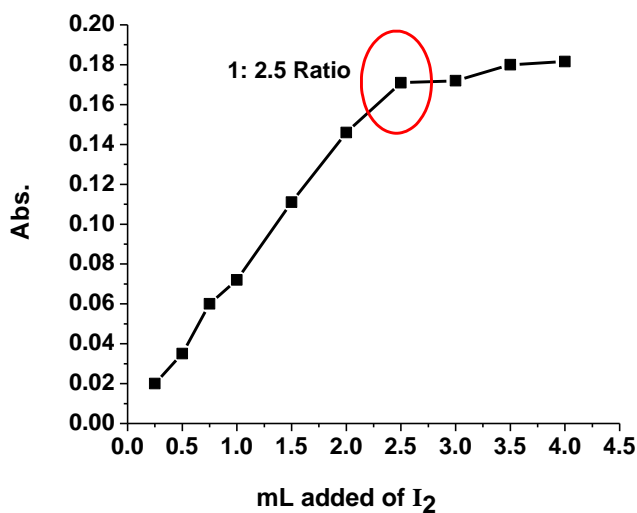


Figure 3. Photometric titration curve of PPD-I₂ system in CHCl₃ at 360 nm

The electronic absorption spectrum of PPD-PA charge-transfer complex was measured in a pure grade of chloroform solvent. The CT complex is formed by adding X ml of 5.0×10^{-4} M picric acid acceptor where (X = 0.25, 0.50, 0.75, 1.00, 1.50, 2.00, 2.50, 3.00, 3.50 and 4.00 mL) to 1.00 ml of 5.0×10^{-4} M of PPD donor. The total volume of each system was completed to 5 mL with CHCl_3 solvent. The concentration of PPD in the reaction mixture was kept fixed at 1.00×10^{-4} M in CHCl_3 solvent, while the concentration of PA was varied over the range of 0.25×10^{-4} M to 4.00×10^{-4} M for PPD-PA system in CHCl_3 solvent. These concentrations produce PPD: PA ratios extending along the range from 1:0.25 to 1:4.00. The electronic absorption spectrum of the 1:2 ratio in chloroform is shown in Fig. 4. The spectrum reveals the characterization of the real absorption bands which are not present in the spectra of free reactants. This band is assigned at 419 nm due to the PPD-PA CT complex formed in the reaction of PPD with PA in CHCl_3 solvent. Photometric titration curve based on these characterized absorption band is given in Fig. 5. This photometric titration curve was obtained according to well known methods [40] by the plot of the absorbance against the X ml added of the PA as π -acceptor. The equivalence point shown in this curve clearly indicates that the formed CT complex between PPD and picric acid is 1:2. It was of interest to observe that the solvent has a pronounced effect on the spectral intensity of the formed $[(\text{PPD})(\text{PA})_2]$ complex. The 1:2 modified Benesi-Hildebrand equation [41] was used in the calculations.

$$\frac{C_A^{o^2} C_D^o}{A} = \frac{1}{K\varepsilon} + \frac{1}{\varepsilon} \cdot C_A^o (4C_D^o + C_A^o) \dots\dots\dots (1)$$

Where C_A^o and C_D^o are the initial concentration of the PA acceptor and PPD donor, respectively, and A is the absorbance of the CT-band. The symbol of both K and ε are referring to formation constant and molar extinction coefficient, respectively. The data obtained of $C_A^o (4C_D^o + C_A^o)$ and $(C_A^{o^2} \cdot C_D^o)/A$ in CHCl_3 are plotting in Fig. 6, the straight lines were obtained with a slope of $1/\varepsilon$ and intercept of $1/k\varepsilon$ as shown in Fig. 6. The oscillator strength f was obtained from the approximate formula given in Equation (2) [42]

$$f = (4.319 \times 10^{-9}) \varepsilon_{\max} \cdot \nu_{1/2} \dots\dots\dots (2)$$

Where $\nu_{1/2}$ is the band-width for half-intensity in cm^{-1} . The oscillator strength values together with the corresponding dielectric constants, D , of the solvent used are given in Table 1. The trend of the values in this table reveals two facts: The $[(\text{PPD})(\text{PA})_2]$ shows high values of both the equilibrium constant (K) and the extinction coefficient (ε). This high value of K reflects the high stability of the PPD-PA charge-transfer complex as a result of the expected high donation of the PPD consequently high value of ε which is known to have a high absorptivity values [43-46]. The transition dipole moment (μ) of the PPD complex (Table 1) has been calculated from Equation (3) [45].

$$\mu = 0.0958[\varepsilon_{\max} \nu_{1/2} / \nu_{\max}]^{1/2} \dots\dots\dots (3)$$

Where $\nu_{1/2}$ is the bandwidth at half-maximum of absorbance, ε_{\max} and ν_{\max} are the extinction coefficient and wavenumber at maximum absorption peak of the PPD-PA charge-transfer complex, respectively. The ionization potential (I_p) of the free PPD donor was determined from the CT energies of the CT band of its picric acid complex using the following relationships derived by Aloisi and Piganatro [47, 48].

$$I_D (ev) = 5.76 + 1.53 \times 10^{-4} \nu_{CT} \dots\dots\dots (4)$$

Where E_{CT} is the energy of the CT of the PPD complex, the energy of the $\pi-\pi^*$ or $n-\pi^*$ interaction (E_{CT}) is calculated using Equation (5) [46]

$$E_{CT}(ev) = (h\nu_{CT})= 1243.667 / \lambda_{CT} (nm) \dots\dots\dots (5)$$

Where, λ_{CT} is the wavelength of the complexation band. Determination of resonance energy (R_N), from Briegleb and Czekalla [49] theoretically derived the relation given in Equation (6)

$$\epsilon_{max} (l.mol^{-1}.cm^{-1}) = 7.7 \times 10^4 / [h\nu_{CT} / [R_N] - 3.5] \dots\dots\dots (6)$$

Where ϵ_{max} is the molar extinction coefficient of the complex at the maximum CT absorption, ν_{CT} is the frequency of the CT peak, and R_N is the resonance energy of the complex in the ground state, which obviously is a contributing factor to the stability constant of the complex (a ground state property). The value of R_N for the π -acceptor complex under study is given in Table 1. The standard free energy change of complexation (ΔG°) was calculated from the association constants by Equation (7) [50]

$$\Delta G^\circ = - 2.303 RT \log K_{CT} \dots\dots\dots (7)$$

where ΔG° is the free energy change of the PPD-PA complex ($KJ mol^{-1}$), R is the gas constant ($8.314 J mol^{-1} K$), T is the temperature in Kelvin degrees ($273 + ^\circ C$), and K_{CT} is the association constant of the PPD-PA complex ($l mol^{-1}$) in different solvents at room temperature, the values thus calculated are represented in Table 1. The data of ΔG° has a negative value according to the higher values of formation constant, and then the formation process of PPD-PA charge transfer complex is exothermic feature reactions.

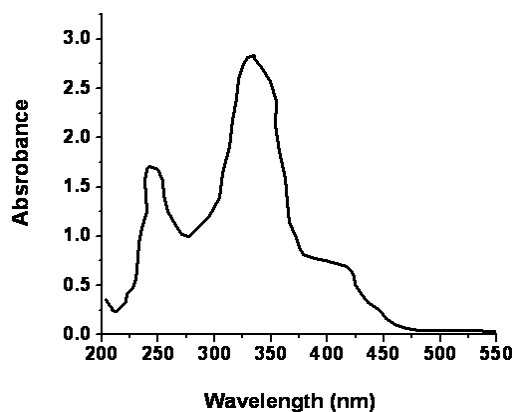


Figure 4. UV-vis absorption spectrum of PPD-PA system in $CHCl_3$ (PPD = 1.0×10^{-4} M and PA = 1.0×10^{-4} M).

Table 1. Spectorphotometric data of the [(PPD)(PA)₂] charge transfer system

λ_{max} (nm)	E_{CT} (eV)	K ($l.mol^{-1}$)	ϵ_{max} ($l.mol^{-1}.cm^{-1}$)	f	μ	I_p	D	R_N	$\Delta G^\circ (25^\circ C)$ $KJmol^{-1}$
419	2.97	1.90E+8	0.07E+4	0.50	7.34	9.41	4.7	2.26E-2	-47237

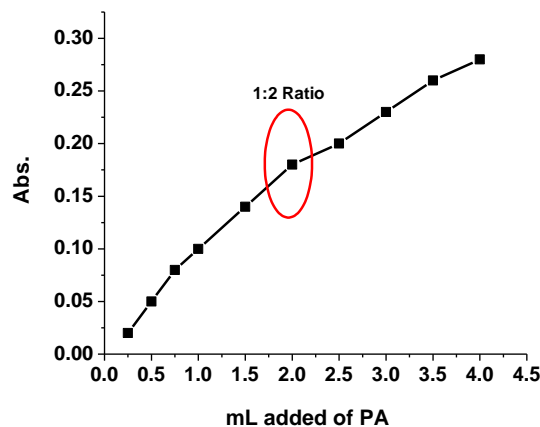


Figure 5. Photometric titration curve of PPD-PA system in CHCl_3 at 419 nm

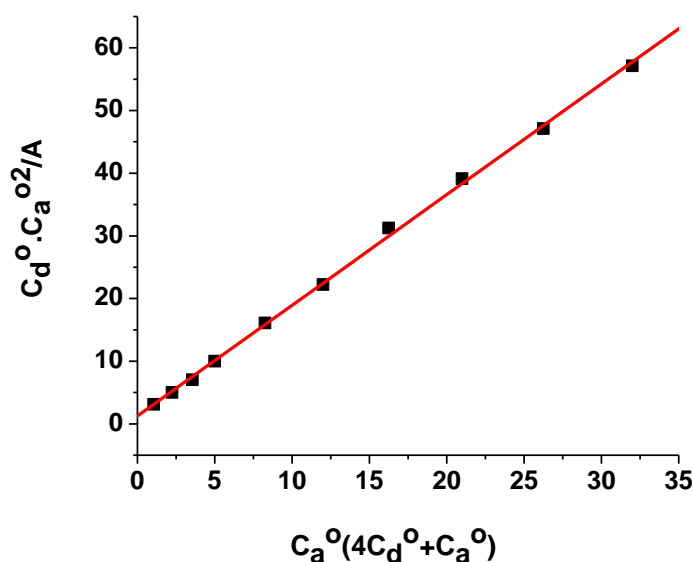


Figure 6. The modified Benesi-Hildebrand plot between $C_a^0(4C_d^0+C_a^0)$ and $C_d^0.C_a^0^2/A$ for the PPD-PA charge transfer system

3.2. Infrared spectra

The infrared spectra of free PPD, $[(\text{PPD})]^+.\text{I}_5^-$, and $[(\text{PPD})(\text{PA})_2]$ charge transfer complexes are shown in Fig. 7a-c and the band assignments are summarized in Table 2. The main characteristic infrared bands of PPD free donor can be summarized as follows: the (asymmetric and symmetric) stretching vibration motions of $-\text{CH}$ aromatic and stretching vibration bands of νCH_2 aliphatic methylene groups are observed at 3066 and $(2956, 2864 \text{ and } 2792) \text{ cm}^{-1}$, respectively. The stretching frequencies bands of the carbonyl groups of the 1,8-naphthalimide molecules $\nu\text{C}=\text{O}$ absorption [51] are observed with very strong intensity bands at 1698 cm^{-1} and 1658 cm^{-1} . In the free PPD donor, the $-\text{C}=\text{C}$ stretching absorption bands at $1624 \text{ and } 1589 \text{ cm}^{-1}$ are due to aromaticity of naphthalene rings. The bending vibrations of $-\text{CH}_2$ groups for the aliphatic PPD donor have some bands at around 1440 cm^{-1} . The $-\text{CH}$ out-of-plane deformation characteristic vibrations bands of the aromatic naphthalene

rings are at 845 and 777 cm^{-1} . The characteristic bands for the C–N bonds due to the tertiary amino group from aliphatic PPD donor and C–N–C imide group from 1,8-naphthalimide moiety are at 1347, 1234 and 1195 cm^{-1} . The spectrum of the pentaiodide and picric acid complexes contains the main characteristic bands of PPD (donor) due to the formation of the $[(\text{PPD})]^+ \cdot \text{I}_5^-$, and $[(\text{PPD})(\text{PA})_2]$ charge transfer complexes. The spectra of $[(\text{PPD})]^+ \cdot \text{I}_5^-$, and $[(\text{PPD})(\text{PA})_2]$ complexes show some difference in wavenumbers and intensities from the free donor PPD (Fig. 7a-c). Obviously, the spectra of $[(\text{PPD})]^+ \cdot \text{I}_5^-$, and $[(\text{PPD})(\text{PA})_2]$ complexes, the absorb C–N groups of the tertiary amino group from aliphatic PPD donor ($\sim 1200 \text{ cm}^{-1}$) show difference (18–38) cm^{-1} compared with those of free PPD, Table 2. This supported that the complexation of PPD with iodine and picric acid takes place through the C–N groups of the tertiary amino group from aliphatic PPD donor rather than the C–N–C imide group from 1,8-naphthalimide moiety (Fig. 8). Also, this is supported by the fact that the vibration of aromatic rings no changes in the spectra of both the free and the complexes Table 2. The other fact is that the nitrogen of sp^3 preferable to make charge transfer complexation rather than nitrogen of sp^2 hybridized. The imide molecule nitrogen looks sp^3 hybridized but it is sp^2 because of conjugation (lone pair goes into a p orbital to have three adjacent, parallel p orbitals) [52].

3.3. Raman laser spectra

Table 2. Infrared frequencies (cm^{-1}) and band assignments of free PPD, $[(\text{PPD})]^+ \cdot \text{I}_5^-$, and $[(\text{PPD})(\text{PA})_2]$ charge transfer complexes

Frequencies (cm^{-1})			Assignments
PPD	$[(\text{PPD})]^+ \cdot \text{I}_5^-$	$[(\text{PPD})(\text{PA})_2]$	
3066	3056	3102	$\nu(\text{C-H})$ arom.
2956, 2864, 2792	2958, 2734	2958, 2926, 2856	$\nu(\text{CH}_2)$
1698	1696	1698	$\nu_{\text{as}}(\text{C=O})$
1658	1653	1653	$\nu_{\text{s}}(\text{C=O})$
1624, 1589	1621, 1587	1628, 1589	$\nu(\text{C=C})$ arom.
1441	1439	1434	$\delta(\text{CH}_2)$
1347, 1234, 1195	1346, 1236, 1177	1344, 1236, 1157	$\nu(\text{C-N})$: tertiary + imide
845, 777	845, 778	844, 777	$\delta(\text{CH})$: out-of-plane
--	--	537	$\delta(\text{NO}_2)$: PA

Table 3. Raman laser characteristic bands of $[(\text{PPD})]^+ \cdot \text{I}_5^-$ charge-transfer complex and two examples of pentaiodide ions with $D_{\infty h}$ (linear) and C_{2v} (nonlinear) symmetry group.

Compounds	Assignments				Symmetry point group
	$\nu_{\text{s}}(\text{I-I})$: outer	$\nu_{\text{s}}(\text{I-I})$: inner	$\nu_{\text{as}}(\text{I-I})$: outer	$\nu_{\text{as}}(\text{I-I})$: inner	
$[(\text{PPD})]^+ \cdot \text{I}_5^-$	146	111	--	--	$D_{\infty h}$ (linear)
$(\text{TMA})_{10}\text{H}^+ \cdot \text{I}_5^-$	162	104	--	--	$D_{\infty h}$ (linear)
$(\text{CH}_3)_4\text{N}^+ \cdot \text{I}_5^-$	160	112	145	74	C_{2v} (nonlinear)

TMA = trimesic acid

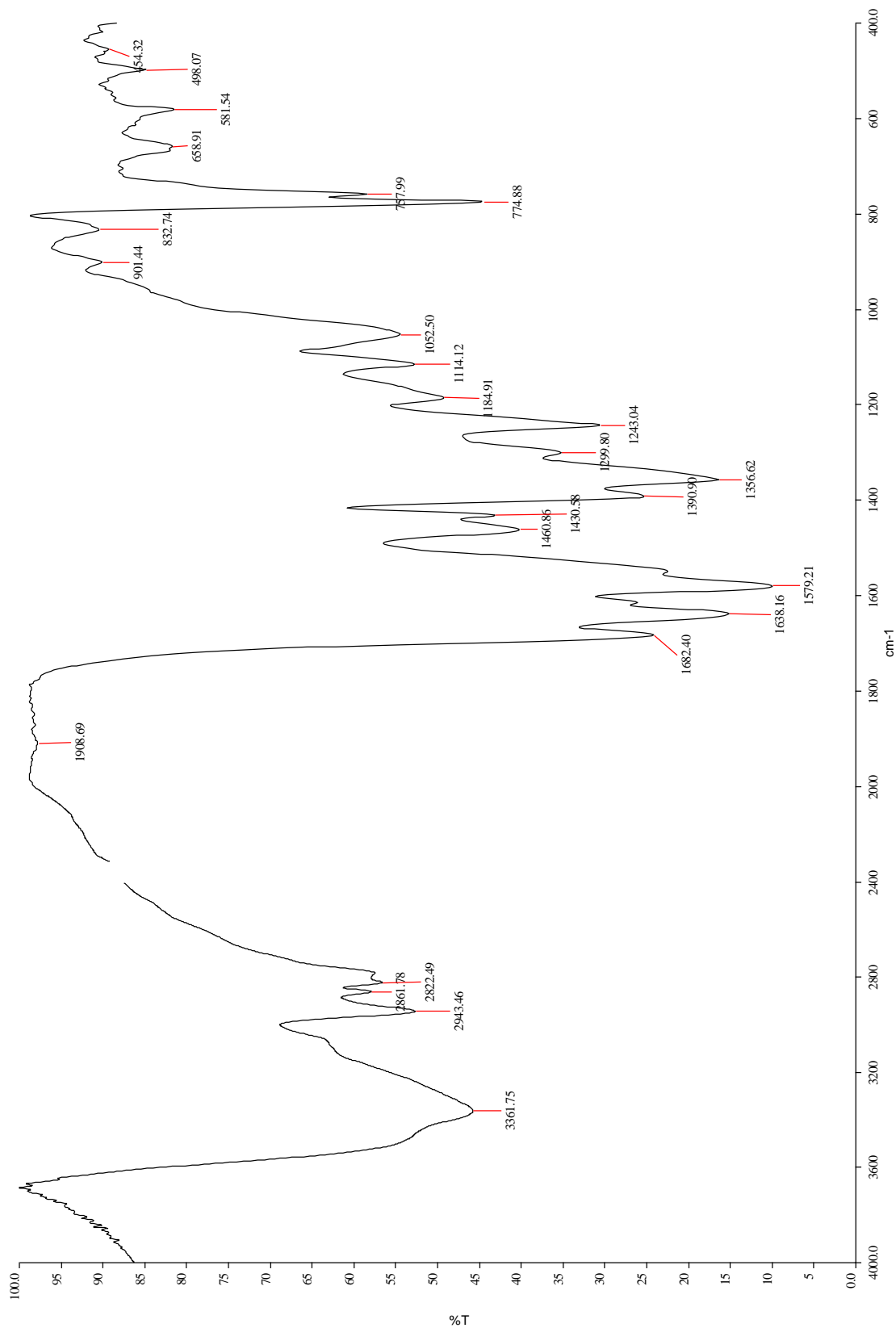


Figure 7a. Infrared spectrum of PPD free donor

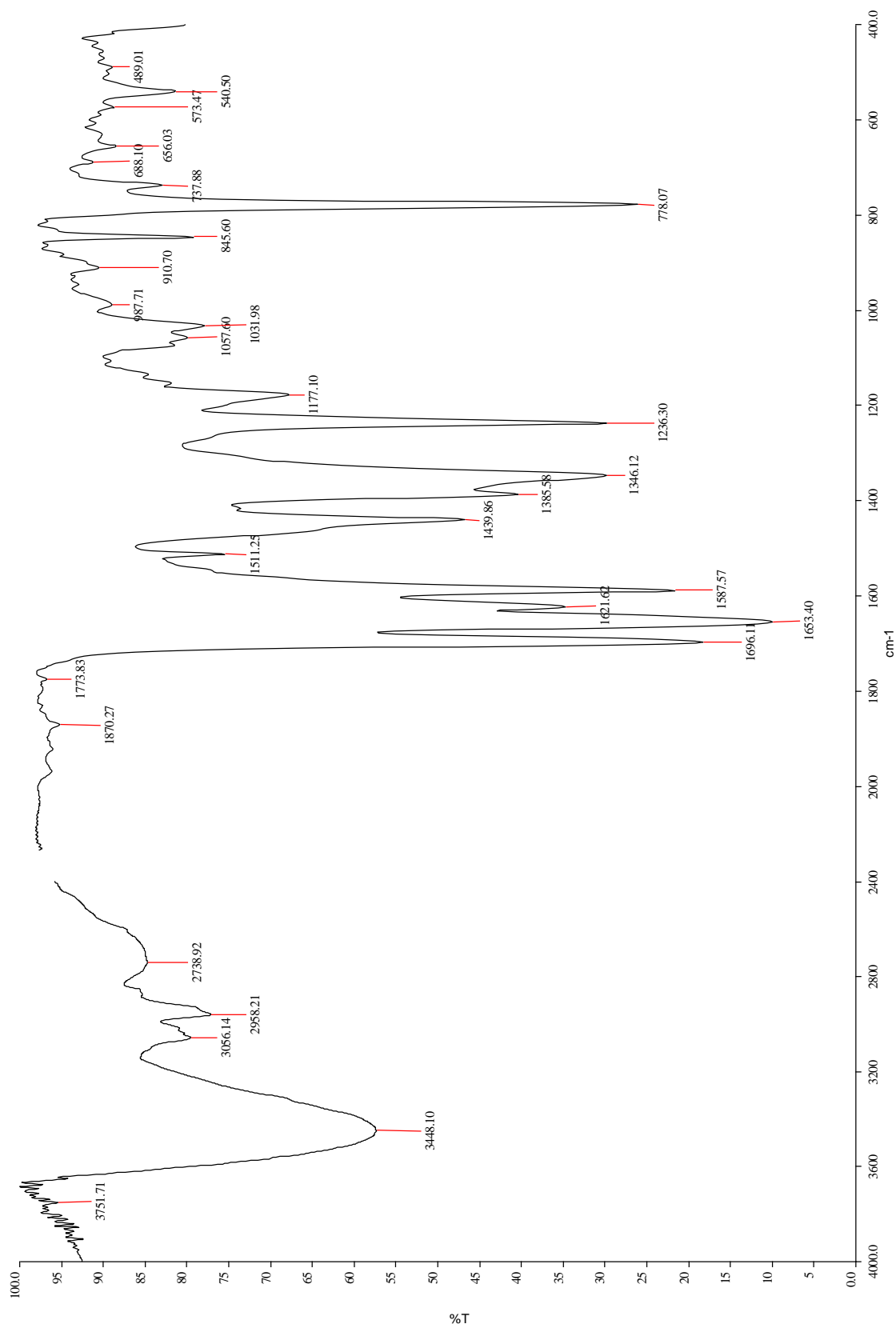


Figure 7b. Infrared spectrum of [(PPD)]⁺.I₅⁻ charge transfer complex

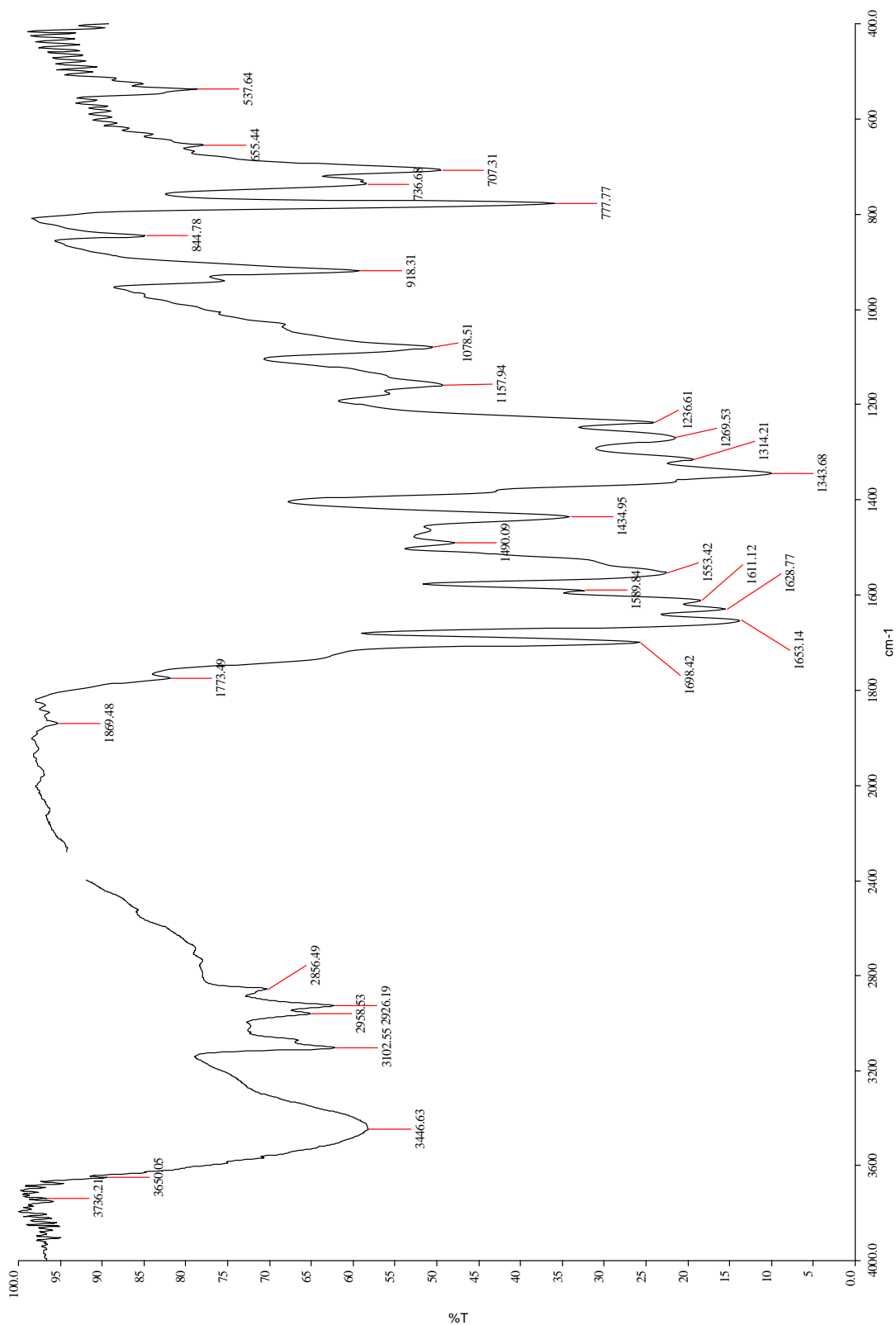


Figure 7c. Infrared spectrum of [(PPD)(PA)₂] charge transfer complex

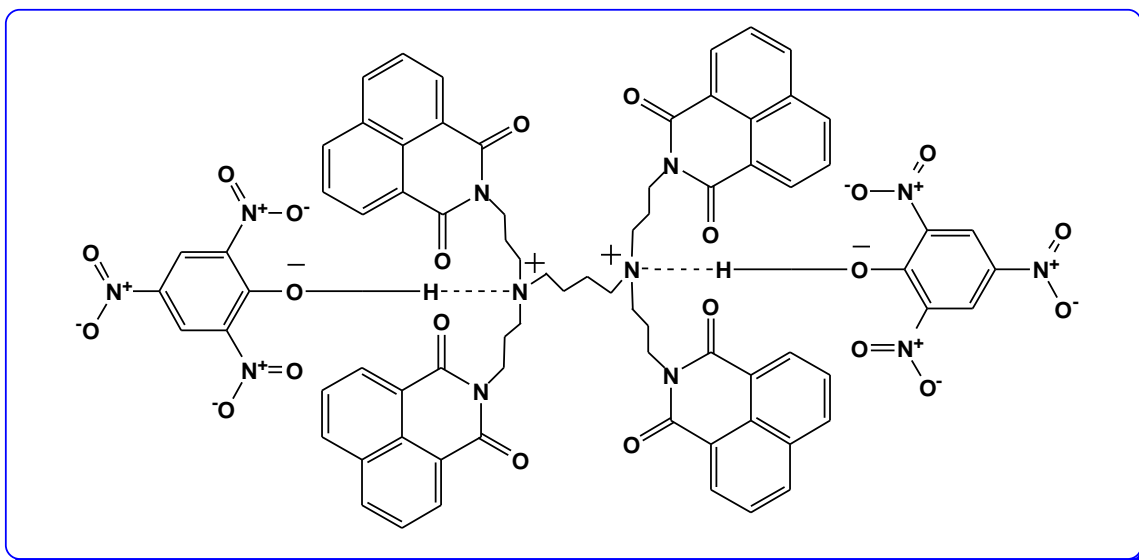


Figure 8. Speculated structure of [(PPD)(PA)₂] charge-transfer complex

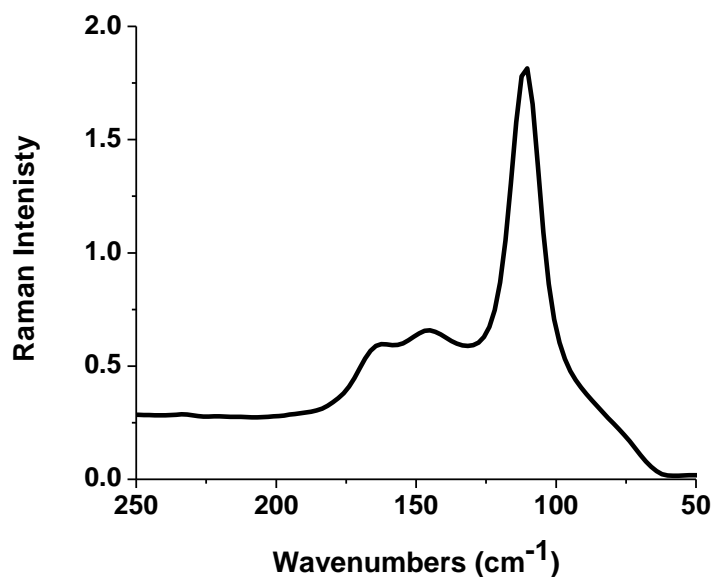


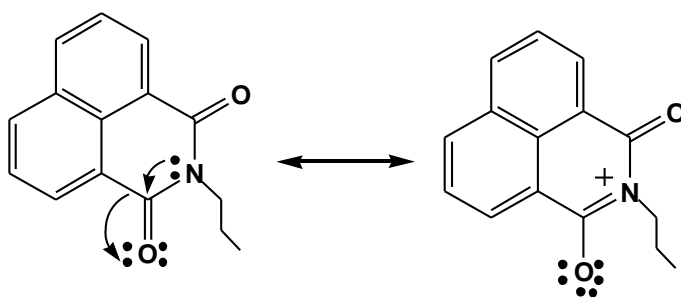
Figure 9. Raman laser spectrum of [(PPD)]⁺.I₅⁻ charge-transfer complex

The Raman spectrum of the solid iodide, [(PPD)]⁺I₅⁻, complex is shown in Fig. 9 and its band assignments are given in Table 3 comparable with symmetry data in literature survey. The pentaiodide ion, I₅⁻ in [(PPD)]⁺I₅⁻ complex has two possibilities as linear (D_{∞h}) or non-linear (C_{2v}) point groups. If the pentaiodide ion I₅⁻ has four active Raman bands within the region 70-165 cm⁻¹ it can be assigned to non-linear C_{2v} symmetry while if the Raman spectrum has two active bands existed at around 150 and 100 cm⁻¹ so it was assigned to linear I₅⁻ with D_{∞h} point group. The experimental data of our study recorded only two active Raman bands in the spectrum of the polyiodide complex [(PPD)]⁺I₅⁻ at 146

and 111 cm^{-1} which matched with linear polyiodide ($D_{\infty h}$ symmetry). The very broadening medium band at 146 cm^{-1} is assigned to the $\nu_s(\text{I-I})$ outer bonds (Σ_g^+ , ν_1), while the band at 111 cm^{-1} is associated to the $\nu_s(\text{I-I})$ inner bonds (Σ_g^+ , ν_2) [28]. It is also of interest to mention here that the I_5^- ion in the complex under study $[(\text{PPD})]^+\text{I}_5^-$ is linear with $D_{\infty h}$ symmetry similar to $[(\text{TMA})_{10}]\text{H}^+\text{I}_5^-$ and $(\text{CH}_3)_4\text{NI}_5$ that reported in previously study [28].

3.4. $^1\text{H-NMR}$ spectra

The $^1\text{H-NMR}$ spectrum of the $[(\text{PPD})(\text{PA})_2]$ charge-transfer complex in d_6 -dmsO displayed distinct signal with appropriate singlet and multiplets peaks as shown in Fig. 10. $^1\text{H-NMR}$ data of PPD free donor $\delta(\text{ppm}) = 1.24(\text{m}, 12\text{H}, \text{N-CH}_2\text{-CH}_2)$, $2.18(\text{t}, 12\text{H}, \text{CH}_2\text{-N}(\text{CH}_2)\text{-CH}_2)$, $4.13(\text{t}, 8\text{H}, \text{CH}_2\text{-N}$ of naphthalamide), and $7.74(\text{m}, 8\text{H}, \text{Ar-H})$, $8.31(\text{m}, 16\text{H}, \text{Ar-H})$. For the $[(\text{PPD})(\text{PA})_2]$ charge-transfer complex, $^1\text{H-NMR}$ data $\delta(\text{ppm}) = 0.923\text{-}1.752$ (m, 12H, N-CH₂-CH₂), 2.118-3.293 (t, 12H, CH₂-N(CH₂)-CH₂), 4.128-4.400 (t, 8H, CH₂-N of naphthalimide), 7.748-7.885 (m, 8H, Ar-H), and 8.410-8.628 (m, 16H, Ar-H), there is no difference in places of the signals in comparison with PPD free donor except for the shifted to lower value concerning of protons attached to C-N groups of the tertiary amino group from aliphatic also there are decreasing in the intensities according to electronic configuration of the new complex. The lone pair allows the nitrogen to act like a Lewis Base, which is it has electrons that it can donate to an electron deficient species. The greater the p-orbital character of the amine the greater the basicity. Therefore sp^3 hybridized nitrogens are more basic than sp^2 hybridized nitrogens. 1,8-naphthalimide is not basic since the lone pair on the nitrogen is involved in aromaticity, and is consequently unavailable. Amides are nonbasic since there is resonance stabilization with the oxygen that removes electron density from the nitrogen (Formula 1). These data are well agreement with the infrared data which supported the place of charge-transfer complexation through the migration of protons ($-\text{OH}$ of phenolic group of acceptor) from acidic centers to sp^3 nitrogen atom which is more basicity than sp^2 nitrogen of imide group.



Formula 1. The conjugation system take place in 1,8-naphthalimide molecule

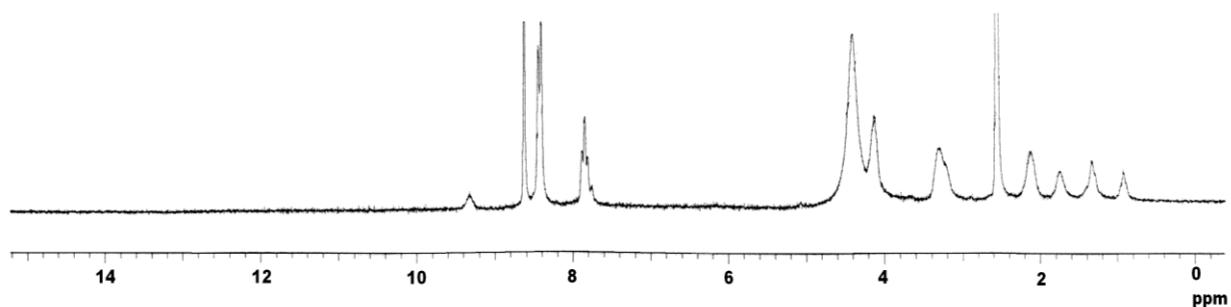


Figure 10. $^1\text{H-NMR}$ spectrum of $[(\text{PPD})]^+.\text{I}_5^-$ charge-transfer complex

3.5. Thermal analyses TG/DTG/DSC

The Poly(propylene amine) dendrimer PPD donor of the first generation is melt at $192\text{ }^\circ\text{C}$ with seven maximum DSC_{max} peaks one of them exothermic at $183\text{ }^\circ\text{C}$ and the other six peaks are endothermic with simultaneous at $361, 389, 414, 419, 428$ and $438\text{ }^\circ\text{C}$, respectively as shown in Fig. 11. The main DTG_{max} peaks were observed at 350 and $547\text{ }^\circ\text{C}$ for PPD from the TG profile (Fig. 12), it appears that the sample decomposes in two sharp stages over the wide temperature rang $25\text{-}600\text{ }^\circ\text{C}$. The decomposition occurs with a mass loss (calcd.: 94.30% , found: 94.41%).

The TG/DTG curves of $[(\text{PPD})]^+.\text{I}_5^-$ charge-transfer complex are shown in Fig. 12. The mass loss (92.23%) between $30\text{-}600\text{ }^\circ\text{C}$ corresponding to the very strong broadening endothermic peak at $298\text{ }^\circ\text{C}$ is due to fully decomposition.

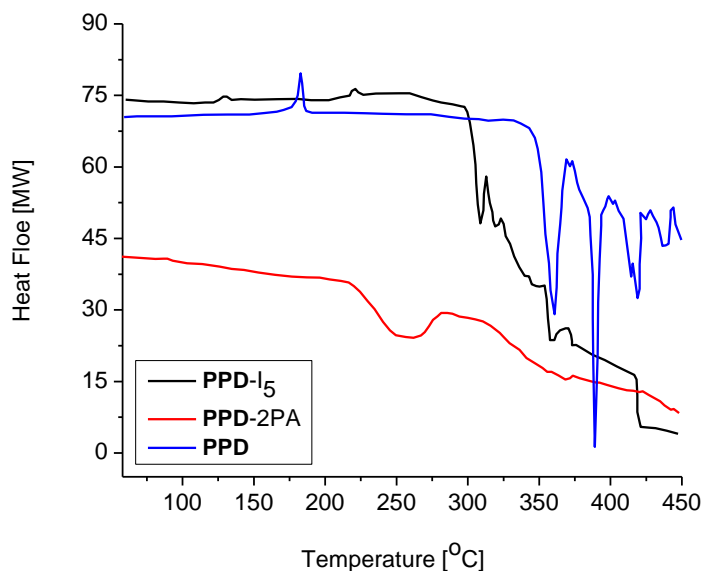


Figure 11. DSC curves of PPD, $[(\text{PPD})]^+.\text{I}_5^-$ and $[(\text{PPD})(\text{PA})_2]$ charge-transfer complexes

The thermal calculations based on the mass loss up to the final temperature are in agreement with the formation of few carbon atoms as the final residual. Figure 11, show the DSC curve for poly(propylene amine) dendrimer of penta iodide complex under nitrogen atmosphere at heating rate 10

$^{\circ}\text{C min}^{-1}$. The DSC two exothermic events at 131 and 221 $^{\circ}\text{C}$ but four endothermic peaks at 309, 320, 348 and 358 $^{\circ}\text{C}$ corresponding to degradation of both poly(propylene amine) dendrimer donor and polyiodide molecules. The final products are carbon atoms as residue, interpretive for no sufficiently of oxygen atoms encouraged the liberated carbon as carbon monoxide or dioxide.

The TG/DTG curves of [(PPD)(PA)₂] charge-transfer complex are shown in Fig. 12. The mass loss (71.35%) between 30-600 $^{\circ}\text{C}$ corresponding to three endothermic peaks at 95 (30-120 $^{\circ}\text{C}$), 210 (120-225 $^{\circ}\text{C}$) and 264 $^{\circ}\text{C}$ within 225-350 $^{\circ}\text{C}$ is due to totally decomposition. The thermal calculations based on the mass loss up to the final temperature are in agreement with the formation of few carbon atoms as the final residual 28.65%. The large percentage of residual carbon atoms due to decomposition of two picric acid acceptors and PPD molecules which has many carbon atoms needed efficiency of oxygen atmosphere. Figure 11, show the DSC curve for poly(propylene amine) dendrimer of picric acid complex under nitrogen atmosphere at heating rate 10 $^{\circ}\text{C min}^{-1}$. The DSC curve has two only clearly appearance endothermic peaks at 251 and 369 $^{\circ}\text{C}$ corresponding to the loss of two picric acid acceptor molecules and large part of PPD organic compound. The few carbon atoms is a residual products in all PPD charge transfer complexes due to the lack of an abundance of oxygen atoms correspond to the large number of carbon atoms present in the super organic molecule of PPD donor and also of π -acceptor. It so difficult to locate units liberated thermally at every decomposition steps due to the convergence of severe between thermal degradation steps, but we can say that the particles terminal is starting to be free before main nuclei and this is clear from the small values of the weight loss in the initial decomposition steps in thermogravimetric curves which expressed the loss in weight with gain increased temperature.

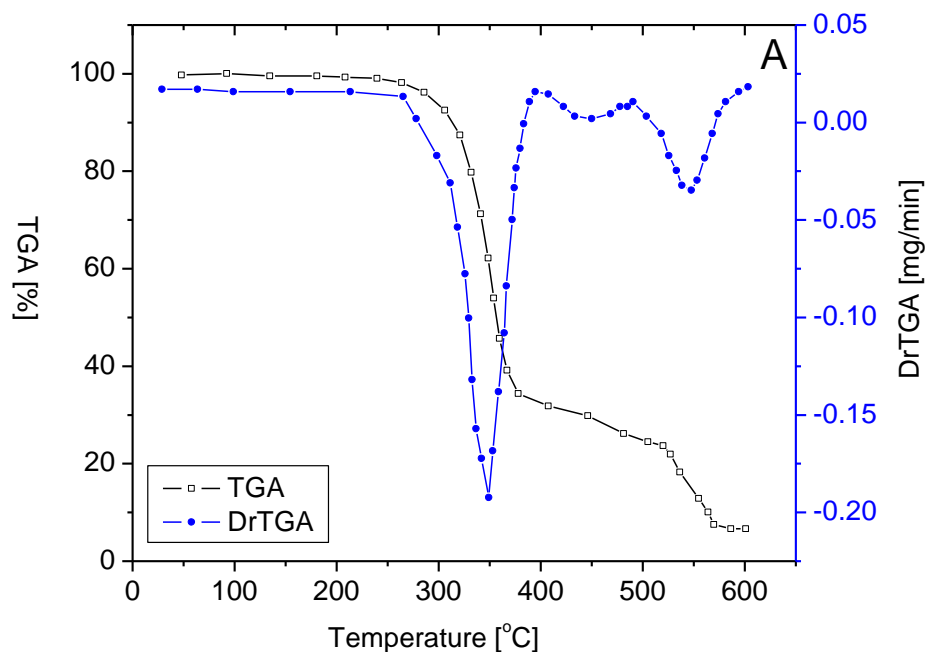


Figure 12A. TG-DTG curves of PPD free donor

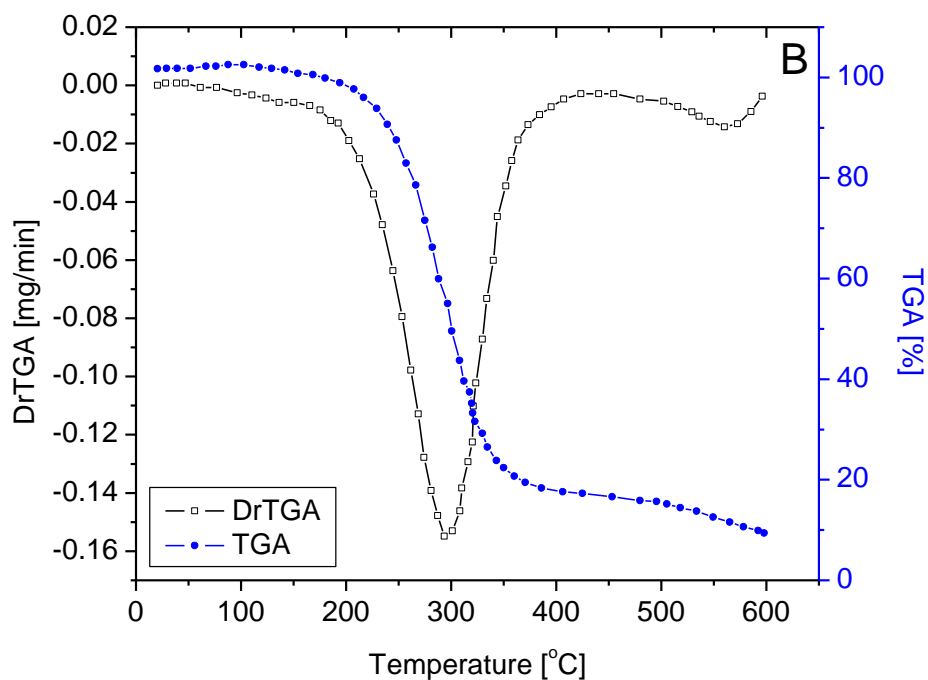


Figure 12B. TG-DTG curves of $[(PPD)]^+ \cdot I_5^-$ charge-transfer complex

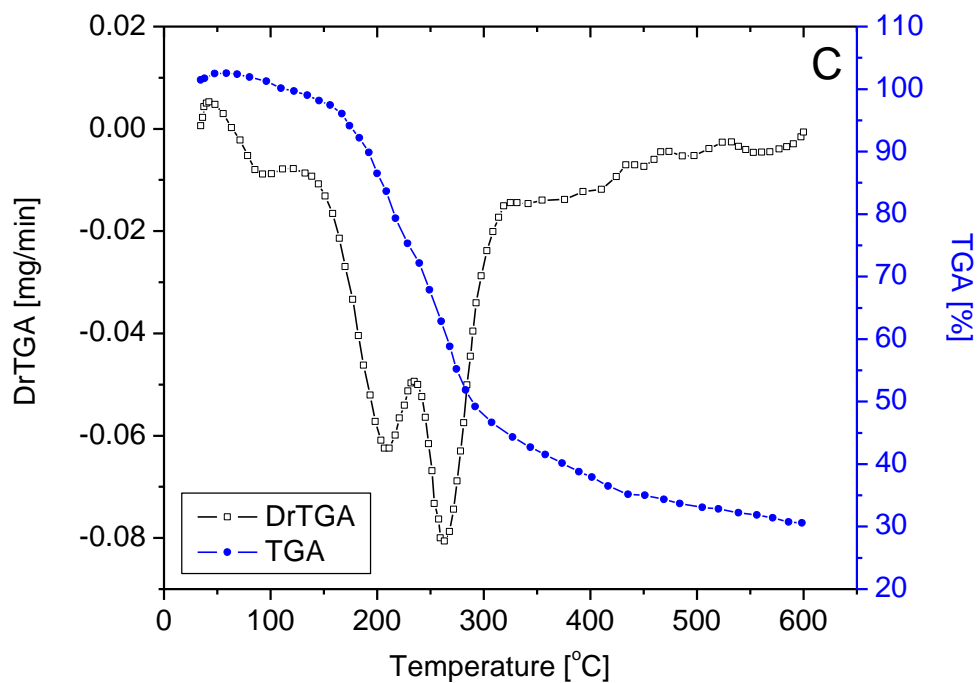


Figure 12C. TG-DTG curves of $[(PPD)(PA)_2]$ charge-transfer complex

References

1. M.W.P.L. Baars, E.W. Meiger, *Topics Cum Chem.* 210 (2000) 131.
2. V. Balzani, PiCeroni, M. Maestri, Ch. Saudan, *Topics Current Chem.* 228 (2003) 159.

3. G.R. Newkome, C.D. Shreiner, *Polymer* 49 (2008) 1.
4. A.P. de Silva, N.Q.N. Gunatratne, T. Gunnlaugsson, A.J.M. Huxley, C.P. McCoy, J.T. Radmancher, *Chem Rev.*, 97 (1997) 1515.
5. L. Jia, Y. Zhang, X. Guo, X. Qian, *Tetrahedron Lett.*, 45 (2004) 3963.
6. K. Inoue, *Progr. Polym. Sci.* 25 (2000) 453.
7. R. Tekade, P. Kumar, N. Jain, *Chem. Rev.* 109 (2009) 49.
8. V. Balzani, P. Ceroni, M. Maestri, V. Vicinelli, *Curr. Opin. Chem. Biol.* 7 (2003) 657.
9. K. Rurack, *Spectrochim Acta Part A* 57 (2001) 2161.
10. G.R. Newkome, C.D. Shreiner, *Polymer*, 49(1) (2008) 1.
11. A. Dirksen, E. Zuidema, R.M. Williams, L. De Cola, C. Kauffmann, F. Vogtle, A. Roque, F. Pina, *Macromolecules*, 35 (2002) 2743.
12. Balzani V., Ceroni P., Gestermann S., Kauffmann C., Gorka M., Vögtle F., *Chem Commun.*, (2000) 853.
13. A. Dirksen, L. De Cola, *C.R. Chimie*, 6 (2003) 873.
14. V. Balzani, F. Vögtle, *C.R. Chimie*, 6 (2003) 867.
15. F. Vögtle, S. Gestermann, C. Kauffmann, P. Ceroni, V. Vicinelli, L. De Cola, V. Balzani, *J Am. Chem. Soc.*, 121 (1999) 12261.
16. F. Vögtle, S. Gestermann, C. Kauffmann, P. Ceroni, V. Vicinelli, L. De Cola, V. Balzani, *J Am. Chem. Soc.*, 122 (2000) 10398.
17. F. Pina, Passaniti, M. Maestri, V. Balzani, F. Vögtle, M. Gorka, S.-K. Lee, J. Van Heyst, H. Fakhrnabavi, *Chem Phys Chem.*, 5 (2004) 473.
18. I. Grabchev, I.H. Boyaci, U. Tamer, I. Petkov, *International J. Inorg. Chem.*, Volume 2013, Article ID 895956, 6 pages; <http://dx.doi.org/10.1155/2013/895956>
19. I.M. Khan, A. Ahmad, M. Aatif, *J. Photochem. Photobiol. B: Biol.* 105 (2011) 6.
20. M.S. Refat, H.A. Ahmed, I. Grabchev, L.A. El-Zayat, *Spectrochim. Acta A* 70 (2008) 907.
21. M.S. Refat, S.M. Teleb, I. Grabchev, *Spectrochim. Acta A* 61 (2005) 205.
22. M.S. Refat, O.B. Ibrahim, H.A. Saad, A.M.A. Adam, *J. Mol. Struct.* 1064 (2014) 58.
23. H.H. Eldaroti, S.A. Gadir, M.S. Refat, A.M.A. Adam, *Spectrochim. Acta A* 115 (2013) 309.
24. A.M.A. Adam, M.S. Refat, H.A. Saad, *J. Mol. Struct.* 1051 (2013) 144.
25. A.M.A. Adam, M.S. Refat, H.A. Saad, *J. Mol. Struct.* 1037 (2013) 376.
26. I.M. Khan, A. Ahmad, S. Kumar, *J. Mol. Struct.* 1035 (2013) 38.
27. I.M. Khan, A. Ahmad, M.F. Ullah, *Spectrochim. Acta A* 102 (2013) 82.
28. E. M. Nour, L. H. Chen, J. Laane, *J. Phys. Chem.* 90 (1986) 2841.
29. E. M. Nour, L. Shahada, *Spectrochim. Acta* 44A (1998) 1277.
30. P. J. Trotter, P. A. White, *Appl. Spectrosc.* 32 (1978) 323.
31. W. Kiefer, H. J. Bernstein, *Chem. Phys. Lett.* 16 (1972) 5.
32. L. Andrews, E. S. Prochaska A. Loewenschuss, *Inorg. Chem.* 19 (1980) 463.
33. I. Ikemoto, M. Sakairi, T. Tsutsumi, H. Kuroda, I. Harada, M. Tasumi, H. Shirakawa, S. Ikeda, *Chem. Lett.* (1979) 1189.
34. K. Y. Rajpure, C. H. Bhosale, *Chem. Mater. Chem. Phys.* 64 (2000) 70.
35. S. Licht, *Solar Energy Materials; Solar Cells* 38 (1995) 305.
36. M.S. Refat, S.M. Teleb, I. Grabchev, *Spectrochimica Acta Part A*, 61(1-2) (2005) 205.
37. M.S. Refat, A. El-Didamony, I. Grabchev, *Spectrochimica Acta Part A*, 67(1) (2007) 58.
38. I. Grabchev, D. Staneva, J. Chovelon, *Dyes and Pigments*, 85(3) (2010) 189.
39. M.S. Refat, I.M. El-Deen, I. Grabchev, Z.M. Anwer, S. El-Ghol, *Spectrochimica Acta Part A*, 72(4) (2009) 772.
40. D. A. Skoog, *Principle of Instrumental Analysis*, 3rd edn., Saunders College Publishing, New York, USA, 1985, Ch. 7.
41. H.A. Benesi, J.H. Hilderbrand, *J. Am. Chem. Soc.*, 71 (1949) 2703.
42. H. Tsubomura, R. P. Lang, *J. Am. Chem. Soc.* 86 (1964) 3930.

43. W. Kiefer, H. J. Bernstein, *Chem. Phys. Lett.* 16 (1972) 5.
44. L. Andrews, E. S. Prochaska, A. Loewenschuss, *Inorg. Chem.* 19 (1980) 463.
45. K. Kaya, N. Mikami, Y. Udagawa, M. Ito, *Chem. Phys. Lett.* 16 (1972) 151.
46. R. Rathone, S. V. Lindeman, J. K. Kochi, *J. Am. Chem. Soc.* 119 (1997) 9393.
47. G. Briegleb, *Z. Angew. Chem.* 76 (1964) 326.
48. G. Aloisi, S. Pignataro, *J. Chem. Soc. Faraday Trans.* 69 (1972) 534.
49. G. Briegleb, J. Czekalla, *Z. Physikchem. (Frankfurt)* 24 (1960) 237.
50. A. N. Martin, J. Swarbrick, A. Cammarata, *Physical Pharmacy*, 3rd edition. Lee and Febiger, Philadelphia, PA, 1969, p.344.
51. I. Grabchev, V. Bojinov, C. Petkov, *Chem. Heterocyclic Comp.*, 39(2) (2003) 179.
52. K.B. Wiberg, *ACC. Chem. Res.*, 32 (1999) 922.

© 2014 The Authors. Published by ESG (www.electrochemsci.org). This article is an open access article distributed under the terms and conditions of the Creative Commons Attribution license (<http://creativecommons.org/licenses/by/4.0/>).